



**HAL**  
open science

## A Numerical Convergence Study of some Open Boundary Conditions for Euler equations

Clément Colas, Martin Ferrand, Jean-Marc Hérard, Olivier Hurisse, Erwan Le Coupanec, Lucie Quibel

► **To cite this version:**

Clément Colas, Martin Ferrand, Jean-Marc Hérard, Olivier Hurisse, Erwan Le Coupanec, et al.. A Numerical Convergence Study of some Open Boundary Conditions for Euler equations. PROMS, 2020, 10.1007/978-3-030-43651-3\_62 . hal-02422802v2

**HAL Id: hal-02422802**

**<https://hal.science/hal-02422802v2>**

Submitted on 28 Jan 2020

**HAL** is a multi-disciplinary open access archive for the deposit and dissemination of scientific research documents, whether they are published or not. The documents may come from teaching and research institutions in France or abroad, or from public or private research centers.

L'archive ouverte pluridisciplinaire **HAL**, est destinée au dépôt et à la diffusion de documents scientifiques de niveau recherche, publiés ou non, émanant des établissements d'enseignement et de recherche français ou étrangers, des laboratoires publics ou privés.

# A Numerical Convergence Study of some Open Boundary Conditions for Euler Equations

Clément Colas, Martin Ferrand, Jean-Marc Hérard, Olivier Hurisse, Erwan Le Coupanec and Lucie Quibel

5 **Abstract** We discuss herein the suitability of some open boundary conditions. Con-  
sidering the Euler system of gas dynamics, we compare approximate solutions of  
one-dimensional Riemann problems in a bounded sub-domain with the restriction  
in this sub-domain of the exact solution in the infinite domain. Assuming that no  
10 information is known from outside of the domain, some basic open boundary con-  
dition specifications are given, and a measure of the  $L^1$ -norm of the error inside the  
computational domain enables to show consistency errors in situations involving  
outgoing shock waves, depending on the chosen boundary condition formulation.  
This investigation has been performed with Finite Volume methods, using approxi-  
15 mate Riemann solvers in order to compute numerical fluxes for inner interfaces and  
boundary interfaces.

**Key words:** Finite volumes, approximate Riemann solver, open boundary condi-  
tions, Euler equations, compressible flow

**MSC (2010):** 65M08, 65N08, 76N15

---

C. Colas<sup>1,2</sup> · M. Ferrand<sup>1,3</sup> · J.-M. Hérard<sup>1,2</sup> · O. Hurisse<sup>1</sup> · E. Le Coupanec<sup>1</sup> · L. Quibel<sup>1,4</sup>

<sup>1</sup>EDF R&D, MFEE, 6 quai Watier, 78400, Chatou, France

<sup>2</sup>Aix-Marseille Université, I2M, UMR CNRS 7373, 39 rue Joliot Curie, 13453, Marseille, France

<sup>3</sup>CEREA Lab (Ecole des Ponts ParisTech - EDF R&D), 6-8 avenue Blaise Pascal, Cité Descartes, 77420 Champs-sur-Marne, France

<sup>4</sup>Université de Strasbourg, IRMA, UMR CNRS 7501, 7 rue René Descartes, 67084, Strasbourg, France

e-mail: clement.colas@edf.fr, martin.ferrand@edf.fr, jean-marc.herard@edf.fr,  
olivier.hurisse@edf.fr, erwan.lecoupanec@edf.fr, lucie.quibel@edf.fr

## 1 Introduction

20 Concerning computational fluid dynamics, industrial simulations are frequently performed with a partial or total unknown fluid state outside of the computational domain. How are boundary conditions dealt with when no information is known outside? Here the one-dimensional Euler equations governing inviscid compressible fluid flows are considered. The unknowns  $\rho$ ,  $u$ ,  $P$  respectively denote the density, the velocity and the pressure of the fluid, while the momentum is  $Q = \rho u$ . The total energy  $E$  is such that  $E = \rho \left( \frac{u^2}{2} + \varepsilon \right)$ . The internal energy  $\varepsilon(P, \rho)$  is prescribed by the EOS (Equation Of State). In the sequel, we denote by  $\mathbf{W} = (\rho, Q, E)^t$  the conservative variable,  $\mathbf{Y} = (s, u, P)^t$  the non-conservative variable, with  $s$  the entropy, and  $\mathbf{F}(\mathbf{W}) = (Q, Qu + P, (E + P)u)^t$  the flux function, so that the set of governing equations reads:

$$\partial_t \mathbf{W} + \partial_x \mathbf{F}(\mathbf{W}) = 0. \quad (1)$$

The speed of sound, denoted by  $c$ , is such that  $c^2 = \left( \frac{P}{\rho^2} - \frac{\partial \varepsilon(P, \rho)}{\partial \rho} \right) / \left( \frac{\partial \varepsilon(P, \rho)}{\partial P} \right)$ .

There exists a huge literature on open boundary problems [11, 6, 10, 12]. Among these, one pioneering work on boundary conditions for bounded domain may be found in [1]. Actually, the present work addresses the issue of open numerical boundary conditions to get waves outside of the computational domain and can be connected to the work of [7]. The solution of Euler system (1) is sought in  $\mathbb{R} \times (0, T)$ , with time  $T \in \mathbb{R}_+^*$ , without boundary conditions, see [14]. This solution, expected to be known and unique, is denoted by  $\mathbf{W}_{\Omega_\infty}^{exact}(x, t)$  for  $(x, t) \in \mathbb{R} \times (0, T)$ .

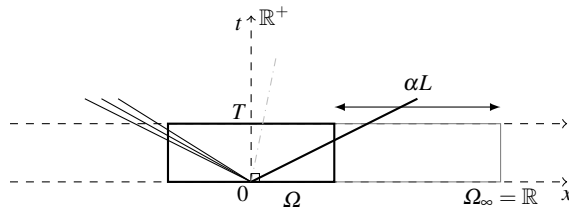


**Fig. 1** Bounded computational domain  $\Omega \subsetneq \Omega_\infty$ , with  $\Omega_\infty$  a spatial infinite domain.

In contrast, the numerical approximations, denoted by  $\mathbf{W}_\Omega^{\Delta x, \Delta t}(x, t)$  for  $(x, t) \in \Omega \times (0, T)$ , are performed in a bounded computational sub-domain  $\Omega \subsetneq \Omega_\infty$  (see Fig. 1) with prescribed open inlet/outlet boundary conditions on  $\partial\Omega$ .

For this purpose, artificial boundaries are introduced on  $\partial\Omega$ . Then, numerical boundary conditions, depending on the time and space steps, must be prescribed on  $\partial\Omega$ . When  $(\Delta x, \Delta t) \rightarrow (0, 0)$ , we assume that some (unique) converged approximation, denoted by  $\mathbf{W}_\Omega^{0,0}(x, t)$  for  $(x, t) \in \Omega \times (0, T)$ , is obtained. Eventually, we wonder whether  $\mathbf{W}_\Omega^{0,0}(x, t)$  for  $(x, t) \in \Omega \times (0, T)$ , coincides with the restriction of

the exact solution to  $\Omega$ ,  $\mathbf{W}_{\Omega_\infty}^{exact}(x, t)$  for  $(x, t) \in \Omega \times (0, T)$ , or not. In the latter case, the converged approximation  $\mathbf{W}_\Omega^{0,0}$  will be said to be **non-consistent**.

For the Euler system (1), a measure of a subsonic state in the last inner cell  $N$  (eigenvalues  $\lambda_1(\mathbf{W}_N^n) < 0$  and  $\lambda_{2,3}(\mathbf{W}_N^n) > 0$ ) at a right outlet will require one scalar external information, whereas in the supersonic case ( $\lambda_{1,2,3}(\mathbf{W}_N^n) > 0$ ), the upwind state will be privileged. Actually, we recall that in the subsonic case, the approach of [4, 5] may provide some way to cope with the lack of information.

A first drawback of the latter approach is that the sign of eigenvalues may easily change: signs of eigenvalues  $\lambda_k(\mathbf{W}_N^n)$  are not necessarily representative of what happens really at the right boundary when computing true waves associated with the 1D Riemann problem with the initial condition:  $\mathbf{W}_L = \mathbf{W}_N^n$  and  $\mathbf{W}_R = \mathbf{W}_{ext}^n$  (unless when  $\mathbf{W}_{ext}^n = \mathbf{W}_N^n$ ). A very instructive example is given in [7] Sect. 3.2, while restricting on a scalar problem (Burgers equation). A second question is: assuming that nothing is known about the exterior state  $\mathbf{W}_{ext}^n$ , how does the solution, inside the computational sub-domain, depend on the choice of  $\mathbf{W}_{ext}^n$ ?

Herein, the aim consists in testing suitable numerical boundary conditions in the sense that they converge towards the – not necessarily regular – exact solution.

## 2 Finite volume method

We briefly recall the basis of the explicit finite volume scheme VFRoe-ncv, an approximate Godunov scheme using non conservative variables [9, 8]. For the sake of simplicity, regular meshes of the one-dimensional computational domain are considered of size  $\Delta x = x_{i+1/2} - x_{i-1/2}$ ,  $i \in \{1, \dots, N\}$ , and  $\Delta t^n = t^{n+1} - t^n$  is the time step,  $n \in \mathbb{N}$ . The time step is given by some CFL condition in order to gain stability.

Let  $\mathbf{W}_i^n$  be an approximation of the mean value  $\frac{1}{\Delta x} \int_{x_{i-1/2}}^{x_{i+1/2}} \mathbf{W}(x, t^n) dx$ . Time-space integration of system (1) over  $[x_{i-1/2}, x_{i+1/2}] \times [t^n, t^{n+1}]$  provides the standard following scheme:

$$\Delta x(\mathbf{W}_i^{n+1} - \mathbf{W}_i^n) + \Delta t^n (\mathbf{g}_{i+\frac{1}{2}}^n - \mathbf{g}_{i-\frac{1}{2}}^n) = 0, \quad (2)$$

where  $\mathbf{g}_{i+1/2}^n$  is the numerical flux through the interface  $\{x_{i+1/2}\} \times [t^n, t^{n+1}]$ . For so-called spatially first-order scheme,  $\mathbf{g}_{i+1/2}^n = \mathbf{g}(\mathbf{W}_i^n, \mathbf{W}_{i+1}^n)$ . The numerical flux  $\mathbf{g}_{i+1/2}^n$  is obtained by solving the linearized Riemann problem:

$$\begin{cases} \partial_t \mathbf{Y} + \mathbf{B}(\tilde{\mathbf{Y}}) \partial_x \mathbf{Y} = 0, \\ \mathbf{Y}(\mathbf{x}, t^n) = \begin{cases} \mathbf{Y}_i^n & \text{if } x < x_{i+\frac{1}{2}}, \\ \mathbf{Y}_{i+1}^n & \text{if } x > x_{i+\frac{1}{2}}, \end{cases} \end{cases} \quad (3)$$

where  $\tilde{\mathbf{Y}} = (\mathbf{Y}_i^n + \mathbf{Y}_{i+1}^n)/2$  and  $\mathbf{B}(\mathbf{Y})$  stands for the following matrix:

$$\mathbf{B}(\mathbf{Y}) = (\partial_{\mathbf{Y}} \mathbf{W})^{-1} \partial_{\mathbf{W}} \mathbf{F}(\mathbf{W}) \partial_{\mathbf{Y}} \mathbf{W} .$$

Once the exact solution  $\mathbf{Y}^* \left( \frac{x-x_{i+1/2}}{t}; \mathbf{Y}_i^n, \mathbf{Y}_{i+1}^n \right)$  of problem (3) is computed, the numerical flux is defined as:

$$\mathbf{g}_{i+1/2}^n = \mathbf{g}(\mathbf{W}_i^n, \mathbf{W}_{i+1}^n) = \mathbf{F}(\mathbf{W}(\mathbf{Y}^*(0; \mathbf{Y}_i^n, \mathbf{Y}_{i+1}^n))) . \quad (4)$$

This numerical flux will be used for both inner interfaces and boundary interfaces.

### 3 Numerical boundary conditions for outgoing waves

80 We propose numerical artificial boundary conditions when no information is given on the open boundary of the computational sub-domain. One possible approach is to determine an artificial state  $\mathbf{W}_{ext}^n$  in the virtual cell, symmetric of the boundary cell  $\mathbf{W}_i^n$ , outside of the sub-domain. The numerical boundary flux is then obtained by  $\mathbf{g}_{1/2}^n = \mathbf{g}(\mathbf{W}_{ext,1}^n, \mathbf{W}_1^n)$  and  $\mathbf{g}_{N+1/2}^n = \mathbf{g}(\mathbf{W}_N^n, \mathbf{W}_{ext,N}^n)$ . In the following, we assume  
85 that the exterior state is connected to the interior state either by a rarefaction wave or a shock wave.

#### 3.1 Outgoing rarefaction wave

##### a. Formulation assuming the invariance of the interior state $\text{BC}_0$

The first boundary condition, widely used in industrial simulations, simply consists  
90 in taking the interior state  $\mathbf{W}_i^n$  of the boundary cell at each time step  $t^n$

$$\mathbf{W}_{ext}^n = \mathbf{W}_N^n . \quad (5)$$

The numerical boundary flux thus reads  $\mathbf{g}_{N+1/2}^n = \mathbf{g}(\mathbf{W}_N^n, \mathbf{W}_N^n) = \mathbf{F}(\mathbf{W}_N^n)$ . This technique does not need any knowledge about the wave structure.

##### b. Formulation using the wave structure and an extrapolation of the interior state $\text{BC}_r$

The second boundary condition is built by using the two associated Riemann invariants of the regular wave and a third additional scalar relation. Note that, for an ideal gas, the exact velocity profile is linear w.r.t.  $x$  at time  $t^n$ . Thus, for an ideal gas EOS such that  $\rho \varepsilon = P/(\gamma - 1)$ , with  $\gamma > 1$ , we get:

$$\rho_{ext}^n = \rho_N^n \left( 1 - \frac{\gamma - 1}{2} \frac{u_{N-1}^n - u_N^n}{c_N^n} \right)^{\frac{2}{\gamma-1}}, \quad P_{ext}^n = P_N^n \left( 1 - \frac{\gamma - 1}{2} \frac{u_{N-1}^n - u_N^n}{c_N^n} \right)^{\frac{2\gamma}{\gamma-1}}$$

and  $u_{ext}^n = 2u_N^n - u_{N-1}^n$ . The numerical boundary flux is computed by  $\mathbf{g}_{N+1/2}^n =$   
95  $\mathbf{g}(\mathbf{W}_N^n, \mathbf{W}_{ext}^n)$ . This technique connects the interior state with the exterior virtual state by using the rarefaction wave structure.

### 3.2 Outgoing shock wave

#### c. Formulation assuming the invariance of the interior state $BC_0$

Same as for rarefaction wave, see case a. (5).

#### 100 d. Formulation using the far-field state $BC_s$

The boundary interior cell  $N$  is connected with the right initial state  $\mathbf{W}_R^0$  by a virtual exterior cell of physical size  $\alpha L$ , with  $L$  the domain length and  $\alpha \in \mathbb{R}_+^*$  a parameter, see Fig. 1. Inspired by [3], this exterior state  $\mathbf{W}_{ext}^n$  is updated with the numerical flux and the known state  $\mathbf{W}_R^0$  such that:

$$\alpha L (\mathbf{W}_{ext}^n - \mathbf{W}_{ext}^{n-1}) + \Delta t^{n-1} (\mathbf{g}(\mathbf{W}_{ext}^{n-1}, \mathbf{W}_R^0) - \mathbf{g}(\mathbf{W}_N^{n-1}, \mathbf{W}_{ext}^{n-1})) = 0. \quad (6)$$

105 This technique gives the following asymptotic update of the exterior state  $\mathbf{W}_{ext}^n$  when  $\alpha \rightarrow +\infty$  for a finite time step  $\Delta t^{n-1}$ :  $\lim_{\alpha \rightarrow +\infty} \mathbf{W}_{ext}^n = \mathbf{W}_{ext}^{n-1}$ . The exterior state is steady and therefore equal to its initial state  $\mathbf{W}_{ext}^0$ , which is the right state  $\mathbf{W}_R^0$ . The numerical boundary flux thus yields:  $\mathbf{g}_{N+1/2}^n = \mathbf{g}(\mathbf{W}_N^n, \mathbf{W}_R^0)$ . This asymptotic boundary condition amounts to impose, in the virtual exterior cell, the right state  
110  $\mathbf{W}_R^0$  known from the initial condition of the Cauchy problem.

## 4 Numerical results

We discuss below some results of this preliminary study. Other results with distinct EOS are available in [2]. Two subsonic test cases, corresponding to 1D Riemann problems with a diatomic ideal gas EOS ( $\gamma = \frac{7}{5}$ ), are performed with CFL= 0.5. The first one is a pure left outgoing 1-rarefaction wave with the initial condition:

$$\begin{cases} (\rho_L, u_L, P_L) = (1 \text{ kg/m}^3, 0 \text{ m/s}, 10^5 \text{ Pa}), \\ (\rho_R, u_R, P_R) = (0.5 \text{ kg/m}^3, 242.2 \text{ m/s}, 3.789 \times 10^4 \text{ Pa}). \end{cases}$$

The second one is a pure right outgoing 3-shock wave with the initial condition:

$$\begin{cases} (\rho_L, u_L, P_L) = (1 \text{ kg/m}^3, 418.3 \text{ m/s}, 2.75 \times 10^5 \text{ Pa}), \\ (\rho_R, u_R, P_R) = (0.5 \text{ kg/m}^3, 0 \text{ m/s}, 10^5 \text{ Pa}). \end{cases}$$

The numerical convergence of the scheme, when waves are gone out of the bounded computational domain  $\Omega = (-200 \text{ m}, 200 \text{ m})$ , is measured with the  $L^1$ -norm of the error.

115 For smooth waves, the boundary conditions  $BC_0$  and  $BC_r$  enable to guarantee consistency when waves are going out ( $t_0 < t < t_1$ ) or are gone out ( $t > t_1$ ) of  $\Omega$ . The numerical errors and the rates of convergence are collected in Table 1 and Fig. 2 for an outgoing rarefaction wave, and in Table 2 and Fig. 3 when the whole rarefaction wave has left the computational domain. As expected for an ideal gas EOS [8], the  
120 numerical rates of convergence for variables  $(u, P)$  are approximately 0.85 – close

to 1 – when  $t < t_1$  (see Table 1), and thus similar to those arising for  $t < t_0$ , see [8, 9]. Table 2 shows greater orders of convergence which may be due to the fact that the exact solution becomes fully constant for  $t > t_1$ . The  $BC_r$  condition gives very similar errors and does not provide more accurate approximations.

125 In contrast, the  $BC_0$  condition does not ensure the consistency of the scheme for an outgoing shock wave (at  $t > t_0$ , shock is outside of  $\Omega$ ), see Fig. 4: clearly, approximate solutions converge towards another solution when  $(\Delta x, \Delta t) \rightarrow (0, 0)$ .

The  $BC_s$  boundary condition, for a finite value of the parameter  $\alpha > 0$ , is still not consistent, see Fig. 5. At the limit  $\alpha \rightarrow +\infty$ , the asymptotic condition  $BC_s$  allows to  
130 retrieve the consistency of the approximate solution with the exact solution.

Further works aim at considering another boundary condition for outgoing shock waves based on an imposed scalar value outside and the Rankine-Hugoniot relations. The issue of the supersonic shock wave case and of the dependence on the scheme [13] are being examined. To our knowledge, this measured loss of consistency has not been pointed out before.

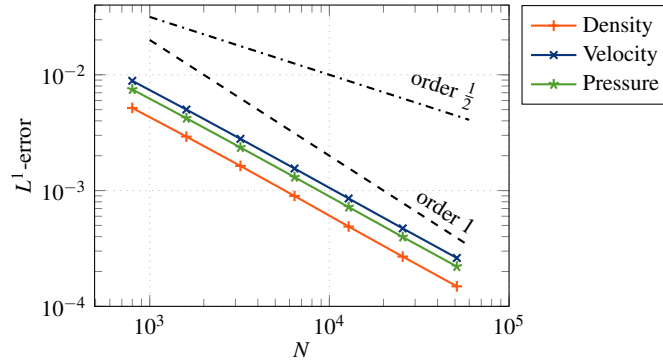
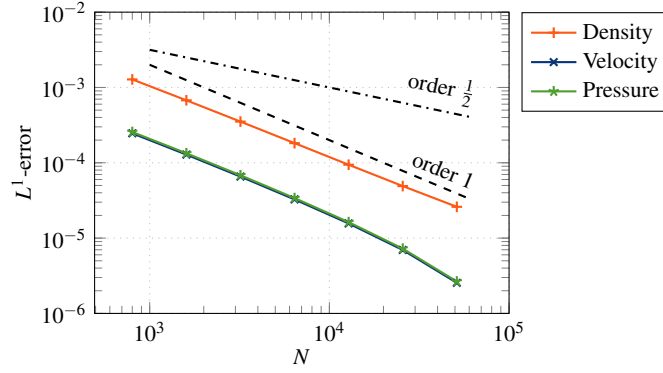


Fig. 2  $BC_0$ :  $L^1$  convergence curves for the rarefaction wave at  $t_0 < t < t_1$ .

Table 1  $BC_0$ :  $L^1$  convergence orders for the rarefaction wave at  $t_0 < t < t_1$ .

| $\Delta x$ (m) | $N$   | $\rho$ $L^1$ -error | $\rho$ cvn. order | $u$ $L^1$ -error | $u$ cvn. order | $P$ $L^1$ -error | $P$ cvn. order |
|----------------|-------|---------------------|-------------------|------------------|----------------|------------------|----------------|
| 5e-1           | 800   | 5.172e-3            |                   | 8.868e-3         |                | 2.371e-3         |                |
| 2.5e-1         | 1600  | 2.925e-3            | 0.8221            | 5.009e-3         | 0.8241         | 1.335e-3         | 0.8243         |
| 1.25e-1        | 3200  | 1.631e-3            | 0.8426            | 2.798e-3         | 0.8403         | 7.478e-4         | 0.8402         |
| 6.25e-2        | 6400  | 8.984e-4            | 0.8605            | 1.550e-3         | 0.8518         | 4.194e-4         | 0.8516         |
| 3.125e-2       | 12800 | 4.891e-4            | 0.8774            | 8.548e-4         | 0.8587         | 2.379e-4         | 0.8582         |
| 1.5625e-2      | 25600 | 2.691e-4            | 0.8621            | 4.714e-4         | 0.8588         | 1.386e-4         | 0.8579         |
| 7.8125e-3      | 51200 | 1.489e-4            | 0.8533            | 2.617e-4         | 0.8491         | 8.461e-5         | 0.8474         |



**Fig. 3**  $BC_0$ :  $L^1$  convergence curves for the rarefaction wave at  $t > t_1$ .

**Table 2**  $BC_0$ :  $L^1$  convergence orders for the rarefaction wave at  $t > t_1$ .

| $\Delta x$ (m) | $N$   | $\rho$ $L^1$ -error | $\rho$ conv. order | $u$ $L^1$ -error | $u$ conv. order | $P$ $L^1$ -error | $P$ conv. order |
|----------------|-------|---------------------|--------------------|------------------|-----------------|------------------|-----------------|
| 5e-1           | 800   | 1.279e-3            |                    | 2.462e-4         |                 | 2.562e-4         |                 |
| 2.5e-1         | 1600  | 6.755e-4            | 0.9211             | 1.284e-4         | 0.9384          | 1.337e-4         | 0.9383          |
| 1.25e-1        | 3200  | 3.522e-4            | 0.9395             | 6.557e-5         | 0.9700          | 6.826e-5         | 0.9700          |
| 6.25e-2        | 6400  | 1.823e-4            | 0.9502             | 3.265e-5         | 1.0061          | 3.399e-5         | 1.0061          |
| 3.125e-2       | 12800 | 9.423e-5            | 0.9521             | 1.565e-5         | 1.0608          | 1.629e-5         | 1.0609          |
| 1.5625e-2      | 25600 | 4.904e-5            | 0.9420             | 6.962e-6         | 1.1687          | 7.247e-6         | 1.1687          |
| 7.8125e-3      | 51200 | 2.604e-5            | 0.9134             | 2.551e-6         | 1.4486          | 2.655e-6         | 1.4486          |

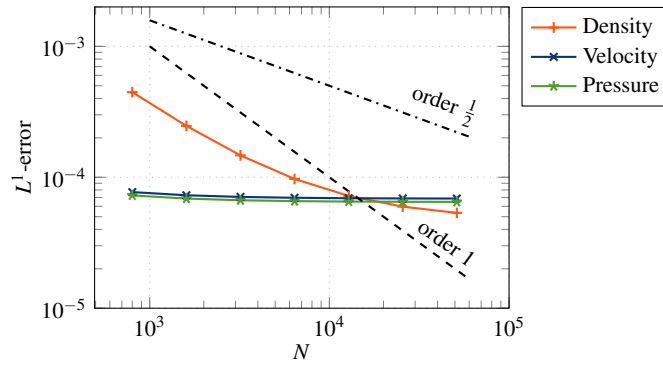


**Fig. 4**  $BC_0$ :  $L^1$  convergence curves for the shock wave at  $t > t_0$ .

**Acknowledgements** The first author received a financial support by ANRT through an EDF-CIFRE contract 2016/0728. The last author also receives a financial support by ANRT through an EDF-CIFRE contract 2017/0476. All computational facilities were provided by EDF R&D.



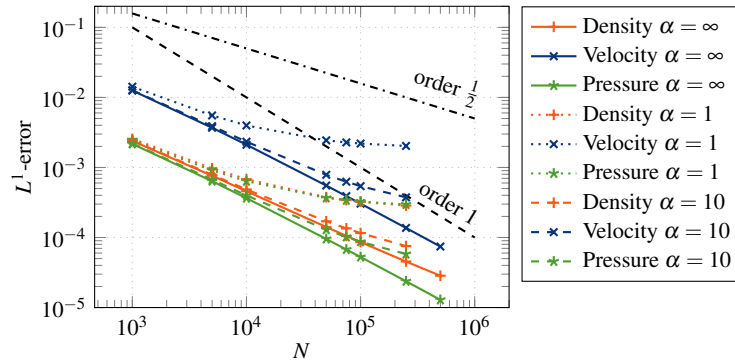


**Fig. 5**  $BC_s$ :  $L^1$  convergence curves for the shock tube at  $t > t_0$ .

## References

- 140 1. Bardos, C., LeRoux, A.Y., Nédélec, J.C.: First order quasilinear equations with boundary conditions. *Communications in Partial Differential Equations* **4**(9), 1017–1034 (1979)
2. Colas, C.: Time-implicit integral formulation for fluid flow modelling in congested media. PhD thesis, Aix-Marseille Université (2019). URL <https://tel.archives-ouvertes.fr/tel-02382958>
- 145 3. Deininger, M., Iben, U., Munz, C.D.: Coupling of three- and one-dimensional hydraulic flow simulations. *Computers & Fluids* **190**, 128 – 138 (2019)
4. Dubois, F.: Boundary conditions and the Osher scheme for the Euler equations of gas dynamics. Internal Report CMAP 170, Ecole Polytechnique, Palaiseau, France (1987)
5. Dubois, F., Le Floch, P.: Boundary conditions for nonlinear hyperbolic systems of conservation laws. *J. Diff Equations* **71**(1), 93–122 (1988)
- 150 6. Engquist, B., Majda, A.: Absorbing boundary conditions for the numerical simulation of waves. *Mathematics of Computation* **31**(139), 629–651 (1977)
7. Gallouët, T.: Boundary conditions for hyperbolic equations or systems. In: M. Feistauer, V. Dolejší, P. Knobloch, K. Najzar (eds.) *Numerical Mathematics and Advanced Applications*, pp. 39–55. Springer Berlin Heidelberg, Berlin, Heidelberg (2004)
- 155 8. Gallouët, T., Hérard, J.M., Seguin, N.: Some recent Finite Volume schemes to compute Euler equations using real gas EOS. *International Journal for Numerical Methods in Fluids* **39**, 1073–1138 (2002)
9. Gallouët, T., Hérard, J.M., Seguin, N.: On the use of symmetrizing variables for vacuum. *Calcolo* **40**(3), 163–194 (2003)
- 160 10. Hedstrom, G.W.: Nonreflecting boundary conditions for nonlinear hyperbolic systems. *Journal of Computational Physics* **30**, 222–237 (1979)
11. Orlanski, I.: A simple boundary condition for unbounded hyperbolic flows. *Journal of Computational Physics* **21**(3), 251–269 (1976)
- 165 12. Poinso, T.J., Lele, S.K.: Boundary conditions for direct simulations of compressible viscous flows. *Journal of Computational Physics* **101**(1), 104–129 (1992)
13. Quibel, L.: Simulation d'écoulements diphasiques eau-vapeur avec un modèle homogène. PhD thesis in preparation, Université de Strasbourg. URL <http://www.theses.fr/s188859>
- 170 14. Smoller, J.: *Shock Waves and Reaction-Diffusion Equations, A Series of Comprehensive Studies in Mathematics*, vol. 258. Springer-Verlag, New York (1994)